Acta Pharmacologica Sinica

www.nature.com/aps

ARTICLE

The small molecule chemical compound cinobufotalin attenuates resistance to DDP by inducing ENKUR expression to suppress MYH9-mediated c-Myc deubiquitination in lung adenocarcinoma

Jia-hao Liu[1], Hui-ling Yang[2,3], Shu-ting Deng[1], Zhe Hu[1], Wei-feng Chen[1], Wei-wei Yan[1], Ren-tao Hou[1], Yong-hao Li[1], Rui-ting Xian[1,4], Ying-ying Xie[1], Yun Su[5], Li-yang Wu[5], Ping Xu[6], Zhi-bo Zhu[1], Xiong Liu[4], Yu-ling Deng[7], Yu-bing Wang[1,8], Zhen Liu[1,4] and Wei-yi Fang[1]

The small molecule chemical compound cinobufotalin (CB) is reported to be a potential antitumour drug that increases cisplatin (DDP) sensitivity in nasopharyngeal carcinoma. In this study, we first found that CB decreased DDP resistance, migration and invasion in lung adenocarcinoma (LUAD). Mechanistic studies showed that CB induced ENKUR expression by suppressing PI3K/AKT signalling to downregulate c-Jun, a negative transcription factor of ENKUR. Furthermore, ENKUR was shown to function as a tumour suppressor by binding to β-catenin to decrease c-Jun expression, thus suppressing MYH9 transcription. Interestingly, MYH9 is a binding protein of ENKUR. The Enkurin domain of ENKUR binds to MYH9, and the Myosin_tail of MYH9 binds to ENKUR. Downregulation of MYH9 reduced the recruitment of the deubiquitinase USP7, leading to increased c-Myc ubiquitination and degradation, decreased c-Myc nuclear translocation, and inactivation of epithelial-mesenchymal transition (EMT) signalling, thus attenuating DDP resistance. Our data demonstrated that CB is a promising antitumour drug and may be a candidate chemotherapeutic drug for LUAD patients.

Keywords: cinobufotalin; ENKUR; MYH9; chemoresistance; lung adenocarcinoma

Acta Pharmacologica Sinica (2022) 43:2687–2695; https://doi.org/10.1038/s41401-022-00890-x

INTRODUCTION

Lung cancer is the second most common cancer and the primary cause of cancer-related mortality worldwide [1, 2]. LUAD is the major histological subtype of lung cancer and accounts for more than 40% of cases [3, 4]. Currently, the treatment strategies for advanced lung cancer are comprehensive regimens composed of chemotherapy, radiotherapy, surgery, immunotherapy and so on [5]. Chemotherapy is one of the most common strategies, as it can be used before or after surgery and is suitable for those who cannot undergo surgery [6]. However, a troublesome problem is that chemoresistance limits the effectiveness of chemotherapy [7]. Although the mechanism of drug resistance has been studied widely at the molecular, cellular and pathological levels, drug resistance still poses a great challenge to curing LUAD [8, 9].

Cinobufotalin (CB) was initially used as a traditional Chinese medicinal preparation extracted from toad venom for administration by injection [10]. Injection of naturally extracted CB has shown tumour-suppressive activity to inhibit tumour development and to improve the prognosis of patients with some cancers, including hepatocellular carcinoma, gastric carcinoma and non-small-cell lung cancer [11–13]. Recently, the small molecule chemical compound CB was reported to significantly suppress cell growth and prolong survival in vivo when used in combination with DDP in nasopharyngeal carcinoma. Interestingly, it has also been shown to increase the sensitivity of NPC cells to DDP [14, 15], and it seems beneficial to study the role of CB in DDP resistance in LUAD.

Here, we demonstrated that CB induces ENKUR expression to suppress resistance to DDP via PI3K/AKT/c-Jun signalling. The upregulated ENKUR interacts with MYH9 and decreases MYH9 expression by suppressing β-catenin/c-Jun-activated MYH9 transcription, thus inhibiting USP7-mediated deubiquitination of c-Myc and inhibiting its nuclear translocation. Our data suggested that CB is a promising drug that increases sensitivity to DDP and may be an adjuvant or alternative chemotherapeutic drug for LUAD patients.

[1]Cancer Center, Integrated Hospital of Traditional Chinese Medicine, Southern Medical University, Guangzhou 510515, China; [2]Cancer Research Institute, School of Basic Medical Sciences, Southern Medical University, Guangzhou 510515, China; [3]School of Pharmacy, Guangdong Medical University, Dongguan 523808, China; [4]Nanfang Hospital, Southern Medical University, Guangzhou 510515, China; [5]Key Laboratory of Protein Modification and Degradation, Basic School of Guangzhou Medical University, Guangzhou 511436, China; [6]Respiratory Department, Peking University Shenzhen Hospital, Shenzhen 518034, China; [7]Department of Chinese Medicine Rehabilitation, Pingxiang People's Hospital, Pingxiang 337055, China and [8]Guangzhou Eighth People's Hospital, Guangzhou Medical University, Guangzhou 510060, China
Correspondence: Yu-bing Wang (wangyubing95117@163.com) or Zhen Liu (narcissus_jane@163.com) or Wei-yi Fang (fangweiyi1975@163.com)
These authors contributed equally: Jia-hao Liu, Hui-ling Yang

Received: 24 August 2021 Accepted: 15 February 2022
Published online: 16 March 2022

MATERIALS AND METHODS

Cell culture

A549 and SPC-A1 cells were donated by Guangzhou Medical University. The cells were cultured in RPMI-1640 medium (Huixiang Biotechnology Co., Ltd, Guangzhou, China) containing 10% foetal bovine serum (Haoyue Biotechnology Co., Ltd, Guangzhou, China) in a humidified chamber at 37 °C with 5% CO_2.

Cell transfection

The ENKUR plasmids and MYH9 plasmids were obtained from GeneChem (Shanghai, China) and Vigene Biosciences (Shandong, China), respectively. SiRNAs for ENKUR, MYH9, and USP7 were designed and synthesised by RiboBio Inc. (Guangzhou, China) (Supplementary Table S1). Cells were transfected with plasmids and/or siRNAs using Lipofectamine 2000 (Invitrogen Biotechnology, Shanghai, China) 8 h after seeding in a cell culture dish. Cells were collected at 24, 48 or 72 h for further experiments.

Lentivirus production and infection

Lentiviral particles overexpressing ENKUR and the control vector were purchased from GeneChem (Shanghai, China). Approximately 8 h after seeding in a cell culture plate, A549 and SPC-A1 cells were infected with these lentiviral particles. The infection efficiency was determined by Western blotting with an anti-ENKUR antibody.

Cell counting Kit-8 (CCK8) assay

For drug sensitivity testing, ~5×10^3 cells were seeded into 96-well plates, and RPMI-1640 medium with different concentrations of CB and/or DDP was added after the cells adhered. After 48 h, 10 μL of CCK8 solution was used to measure cell viability under treatment with different drug concentrations.

Wound healing assay

To evaluate the migration ability, A549 and SPC-A1 cells treated with or without plasmids, siRNA or CB were seeded into six-well plates, and the cell layer was then scratched with a 10 μL pipette tip. Then, 0 h, 24 h and 48 h after the scratch was made, the relative migration distance of these cells was determined by microscopic observation.

Boyden chamber assay

BD Matrigel (BD Biosciences, NJ, USA) and 500 μL of RPMI-1640 medium containing 10% foetal bovine serum were added to the upper and lower chambers, respectively, of Transwell inserts (BD Biosciences, NJ, USA). Approximately 1×10^5 pretreated cells were collected and resuspended in foetal bovine serum-free RPMI-1640 medium and were then added to the upper chamber. The invaded cells were stained with crystal violet solution and imaged under a microscope. The number of cells in five random fields was used for further analysis.

qPCR and RT-PCR

A reverse transcription reagent kit (TaKaRa Bio, Inc., Shiga, Japan) was used to synthesise cDNA from RNA isolated from cells according to the manufacturer's protocols. Specific primers (Supplementary Table S2), RNase-free water and SYBR Green were added to the cDNA template for amplification. qPCR was performed with a Bio-Rad CFX96 system, and RT–PCR was performed with a Bio-Rad T100 system.

Western blot analysis

Western blot analysis was performed as described previously [16, 17]. Protein was harvested from cell lysates, and the concentrations were then determined with a BCA protein assay kit (Thermo Scientific, Waltham, MA, USA). After quantification, proteins were separated by SDS–PAGE and were then transferred to a polyvinylidene fluoride membrane for further immunodetection with specific antibodies. The expression levels of different proteins were determined with a chemiluminescence reagent kit (Thermo Scientific, Waltham, MA, USA). The primary antibodies included anti-E-cadherin, anti-N-cadherin, anti-ENKUR, anti-MYH9, anti-β-catenin, anti-c-Jun, anti-p-PI3K, anti-PI3K, anti-p-AKT, anti-AKT, anti-USP7, anti-c-Myc, anti-ubiquitin, anti-β-actin and anti-GAPDH. The application information for the primary antibodies is summarised in Supplementary Table S3. A Bio-Rad ChemiDoc CRS + Molecular Imager was used to acquire images.

Coimmunoprecipitation (Co-IP) assay

To identify interactions between proteins, Co-IP was performed in cells treated with different plasmids using a Pierce Coimmunoprecipitation Kit (Thermo Scientific, Waltham, MA, USA). According to the protocols, proteins from A549 cells transfected with different overexpression plasmids were collected and quantified. Protein-specific antibodies and IgG were added to 5 mg of protein and incubated at 4 °C overnight. Mass spectrometry and Western blot analysis were performed using the recovered eluted protein.

Chromatin immunoprecipitation (ChIP) assay

To prove that c-Jun is the transcription factor binding to the ENKUR promoter, a ChIP assay was performed in A549 and SPC-A1 cells using a ChIP assay kit (Thermo Scientific, Waltham, MA, USA). Briefly, chromatin was treated with micrococcal nuclease for digestion into DNA fragments after crosslinking and isolation of the cell pellet. For immunoprecipitation, 10 μL of an anti-c-Jun antibody and 2 μL of normal rabbit IgG were added to the reaction system. After incubation at 4 °C on a rocking platform overnight, the recovered eluted DNA fragments were subjected to qPCR and gel electrophoresis.

Immunofluorescence

Before seeding on coverslips in a 24-well plate, A549 cells were transfected with the ENKUR plasmid. After adherence, the cells were washed with PBS twice and were then fixed and permeabilized with paraformaldehyde and Triton X-100 (0.2%). Subsequently, the cells treated with goat serum were incubated with specific antibodies. After ~12 h, the cells were counterstained with DAPI and were then imaged with a confocal fluorescence microscope (Carl Zeiss LSM800).

Cycloheximide (CHX) chase assay

A549 cells with or without ENKUR and MYH9 overexpression were incubated with 20 μmol/L MG132 (Sigma–Aldrich, MO, USA) or left untreated. After 6 h, 50 μg/ml CHX (Abcam, Massachusetts, USA) was added to these cells, and these cells were collected at 0, 20, 40, 60, 80 and 100 min to obtain proteins. Finally, these proteins were quantified and analysed by Western blotting.

Nuclear and cytoplasmic fractionation assay

To extract nuclear and cytoplasmic proteins, nuclear and cytoplasmic extraction was performed with NE-PER@ Nuclear and Cytoplasmic Extraction Kits (Thermo Scientific, Waltham, MA, USA) purchased from Thermo Scientific. Briefly, cells washed twice with PBS were collected and incubated with CER I reagent. After incubation at 4 °C for 10 min, CER II reagent was added, and the sample was then subjected to centrifugation to obtain the cytoplasmic proteins (the supernatant). For nuclear protein extraction, the remaining pellet was suspended in NER reagent at 4 °C and incubated for 40 min. The mixture was centrifuged for 10 min, and the supernatant containing the nuclear proteins was collected. Finally, the quantified nuclear and cytoplasmic proteins were used for further experiments.

Treatment experiments in nude mice

A total of 5×10^6 ENKUR-overexpressing SPC-A1 cells or control cells were intraperitoneally injected into 4-week-old female BALB/

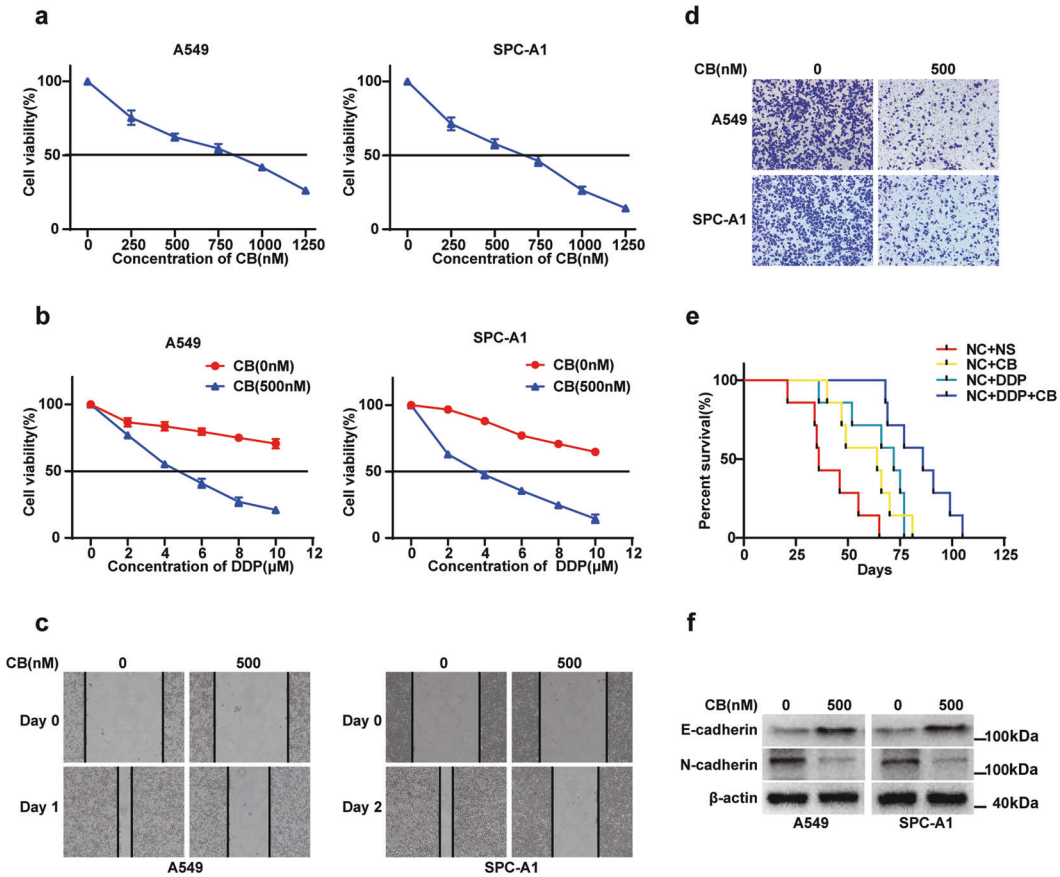

Fig. 1 CB reduces resistance to DDP. a Dose–response curves of LUAD cells to CB at 48 h are shown. **b** The IC_{50} value of DDP in A549 and SPC-A1 cells after treatment with or without CB is shown. Wound healing assays (**c**) and Boyden chamber assays (**d**) were performed in LUAD cells incubated with or without CB. **e** Survival analysis of mice was conducted based on the different treatments. **f** The expression levels of E-cadherin and N-cadherin in CB-treated LUAD cells and control cells are shown.

c-nu mice ($n = 7$ per group). For the CB treatment experiment, the mice injected with control cells were divided into four groups that received different treatments: the normal saline (NS) group, DDP group, CB group and CB + DDP group. To confirm the tumour-suppressive role of ENKUR in vivo, mice injected with ENKUR-overexpressing cells or control cells were divided into four groups: the NC + NS (the same data as above), NC + DDP (the same data as above), ENKUR + NS, and ENKUR + DDP groups. All tumours were allowed to grow for 4 days, and all mice were then intraperitoneally injected with NS, DDP (4 mg/kg) and/or CB (4 mg/kg) every 4 days. The xenograft tumours and the weights of these mice are shown in Supplementary Fig. S1a, b. The survival times were determined after the mice died and were used for Kaplan–Meier survival analysis. The protocols for the mouse experiments conformed to international regulations for animal care and maintenance and were approved by the Institutional Animal Ethical Committee, Experimental Animal Center of Southern Medical University.

Statistical analysis

All data from at least three independent experiments are expressed as the mean ± SD values and were analysed using SPSS 23.0 software (SPSS Inc. Chicago, IL, USA). Student's two-tailed *t* test was used to determine the significance of differences between two groups. Kaplan–Meier survival analysis was used to determine the correlations between different treatments and the survival time of nude mice. All statistical tests were two-sided, and a *P* value of <0.05 was considered to be statistically significant.

RESULTS

CB decreases resistance to DDP

The half-maximal inhibitory concentrations (IC_{50}) in A549 and SPC-A1 cells were 721 nM and 553 nM, respectively, for CB (Fig. 1a) and 24 μM and 17 μM for DDP (Supplementary Fig. S2a). We determined the effects of CB at a concentration of 500 nM. The IC_{50} value of DDP in A549 and SPC-A1 cells was decreased in CB-treated cells compared to negative control cells (Fig. 1b). Wound healing and Boyden chamber assays showed that migration and invasion were attenuated after incubation with CB (Fig. 1c, d and Supplementary Fig. S2b, c). Survival analysis of mice injected intraperitoneally with SPC-A1 cells and subjected to different treatments showed that mice in the DDP group and CB group had longer survival times than mice in the NS group but shorter survival times than mice in the CB + DDP group (Fig. 1e). By Western blotting, we found that CB upregulated E-cadherin and downregulated N-cadherin (Fig. 1f).

ENKUR increases sensitivity to DDP

qPCR and Western blot analysis showed increased mRNA and protein levels of ENKUR in CB-treated A549 and SPC-A1 cells (Fig. 2a, b). To determine the role of ENKUR in chemoresistance, migration and invasion, ENKUR plasmids were transfected into A549 and SPC-A1 cells (Supplementary Fig. S3a). Overexpression of ENKUR was shown to decrease the IC_{50} value of DDP (Fig. 2c) and the migration and invasion abilities of LUAD cells (Fig. 2d, e and Supplementary Fig. S3b, c). In vivo studies demonstrated that ENKUR could increase the survival time in intraperitoneal injection

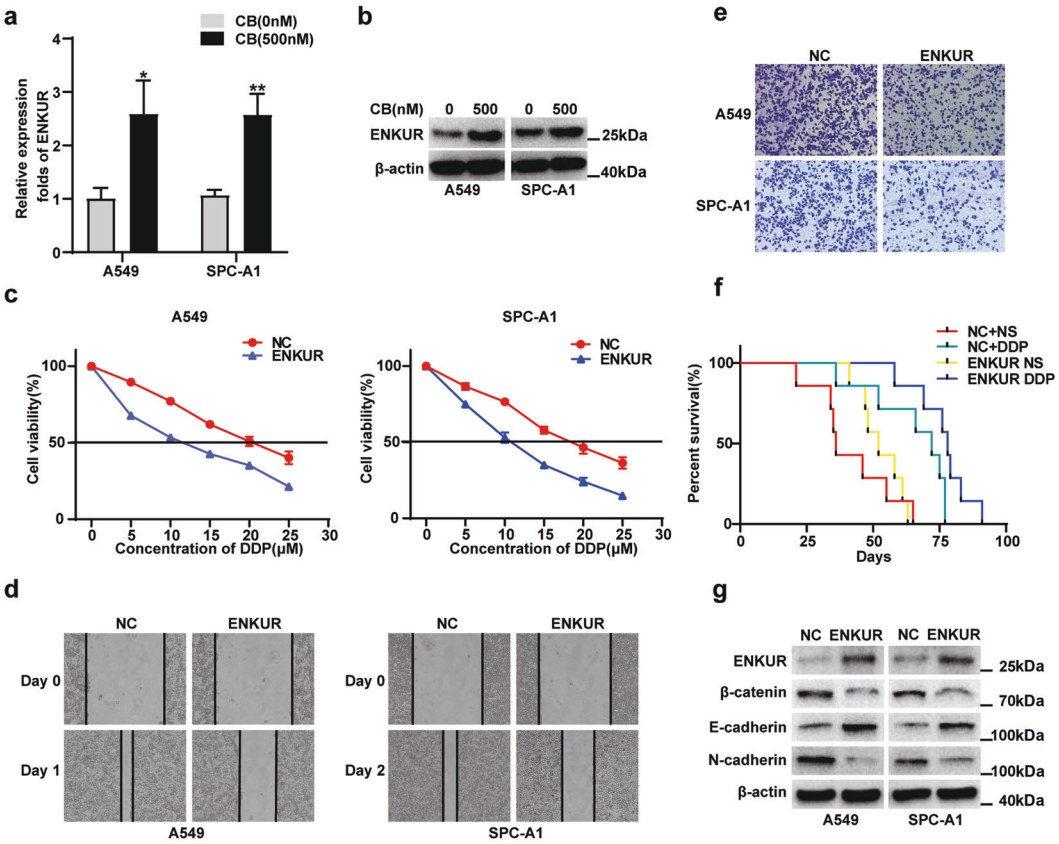

Fig. 2 ENKUR enhances sensitivity to DDP in LUAD. The mRNA (**a**) and protein (**b**) expression levels of ENKUR in CB-treated LUAD cells and control cells are shown. Dose-response curves to DDP (**c**), wound healing assays (**d**) and Boyden chamber assays **(e**) were performed in ENKUR-overexpressing LUAD cells and control cells. **f**. Survival analysis of the mice in the NC + NS group (same data as Fig. 1e), NC + DDP group (same data as Fig. 1e), ENKUR + NS group and ENKUR + DDP group is shown. **g**. Western blot analysis of β-catenin, E-cadherin and N-cadherin in ENKUR-overexpressing A549 and SPC-A1 cells and the corresponding control cells.

models of LUAD. The survival time in the NC + DDP group was longer than that in the NC + NS group and the ENKUR + NS group but shorter than that in the ENKUR + DDP group (Fig. 2f). Mechanistic analysis showed that β-catenin and N-cadherin expression was decreased and E-cadherin expression was increased in ENKUR-overexpressing LUAD cells (Fig. 2g).

Knocking down ENKUR restores resistance to DDP

Decreased ENKUR expression was confirmed in ENKUR-overexpressing LUAD cells transfected with si-ENKUR (Supplementary Fig. S3d). Silencing ENKUR restored both resistance to DDP and the cell migration and invasion abilities in LUAD cells (Supplementary Fig. S3e–g). Transfection with si-ENKUR reversed the β-catenin, E-cadherin and N-cadherin protein expression patterns compared with those in ENKUR-overexpressing A549 and SPC-A1 cells (Supplementary Fig. S3h).

ENKUR binds to MYH9

Mass spectrometry analysis was performed in A549 cells with ENKUR overexpression to identify the proteins interacting with ENKUR, and MYH9 was identified as a candidate interacting protein (Supplementary Table S4). Furthermore, ENKUR was found to bind to MYH9 by a Co-IP assay (Fig. 3a), and colocalization of ENKUR and MYH9 was observed in the cytoplasm of ENKUR-overexpressing A549 cells by an immunofluorescence assay (Fig. 3b). ENKUR contains three domains: an N-terminal region domain, an SH3 domain and an Enkurin domain [18] (Fig. 3c). To verify the specific domain interacting with MYH9, we transfected plasmids containing different domain sequences into A549 cells and observed the interaction between the Enkurin domain and MYH9 (Fig. 3d). Three domains were predicted in MYH9 by InterPro (http://www.ebi.ac.uk/interpro/): Myosin_N, Myosin_head_-motor and Myosin_tail (Fig. 3e). Co-IP assay performed in A549 cells transfected with plasmids containing different domain sequences showed that the Myosin_tail domain was the specific domain interacting with ENKUR (Fig. 3f).

ENKUR suppresses MYH9 expression by suppressing β-catenin/c-Jun

Using qPCR analysis, we observed that the mRNA expression of MYH9 was decreased in ENKUR-overexpressing LUAD cells (Fig. 4a). Our previous studies proved that c-Jun, a negative transcription factor of MYH9, is regulated by β-catenin in HCC [19]. We hypothesised that ENKUR modulates MYH9 expression via β-catenin/c-Jun signalling in LUAD. As expected, overexpression of ENKUR reduced the β-catenin, c-Jun and MYH9 protein levels (Fig. 4b), and transfection of β-catenin restored the c-Jun and MYH9 protein levels in A549 and SPC-A1 cells (Fig. 4c). Co-IP assay showed that ENKUR binds to β-catenin in A549 cells over-expressing ENKUR (Fig. 4d). The result of immunofluorescence assay further confirmed that the interaction between ENKUR and β-catenin occurred in the cytoplasm (Fig. 4e). To determine which domain of ENKUR mediates the interaction between ENKUR and β-catenin, we transfected ENKUR domain plasmids into A549 cells. Co-IP assay performed with these cells demonstrated that the Enkurin domain binds to β-catenin (Fig. 4f).

To further explore the effect of MYH9 on resistance to DDP in ENKUR-overexpressing LUAD cells, MYH9 plasmids were transfected into these cells (Supplementary Fig. S4a). Subsequently, we found that overexpression of MYH9 restored the ENKUR-mediated decreases in DDP resistance, cell migration and invasion, and

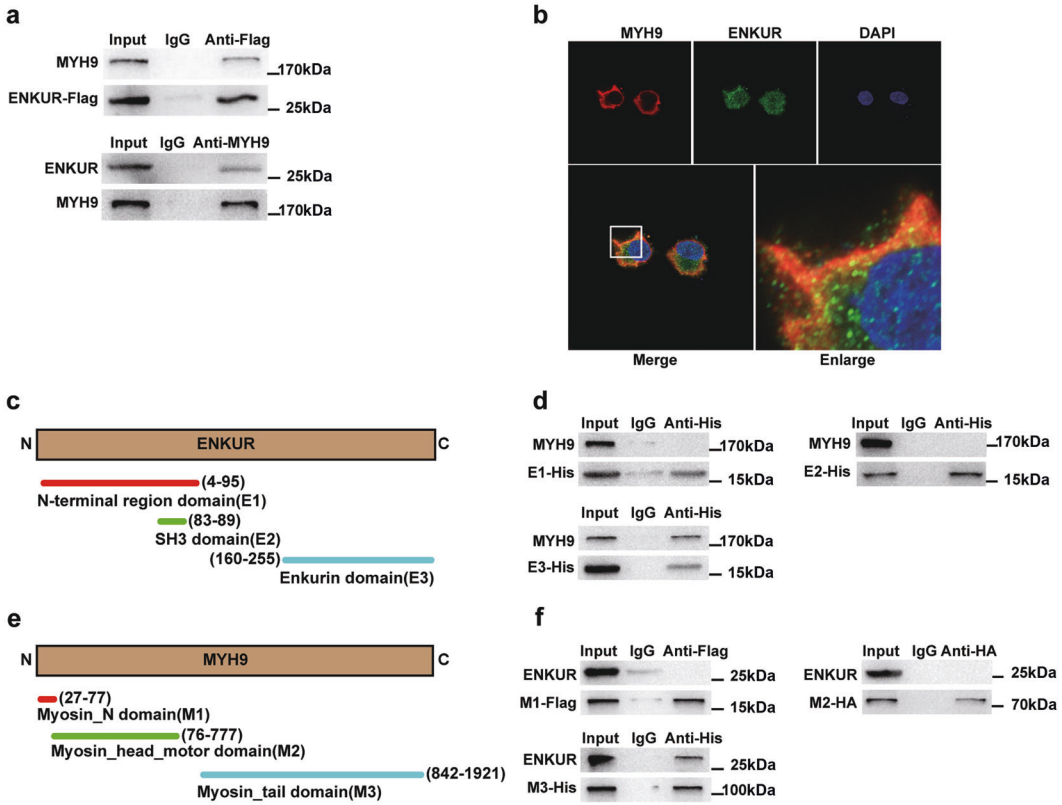

Fig. 3 ENKUR interacts with MYH9. Co-IP (**a**) and immunofluorescence assay (**b**) were utilised to detect the interaction between ENKUR and MYH9 in ENKUR-overexpressing A549 cells. **c** A schematic diagram of the domains in ENKUR is shown. **d** Co-IP was performed in A549 cells transfected with different ENKUR domain plasmids. **e** A schematic diagram of the domains in MYH9 is shown. **f** Coimmunoprecipitation analysis was used to determine the specific domain in MYH9 that binds to ENKUR in A549 cells.

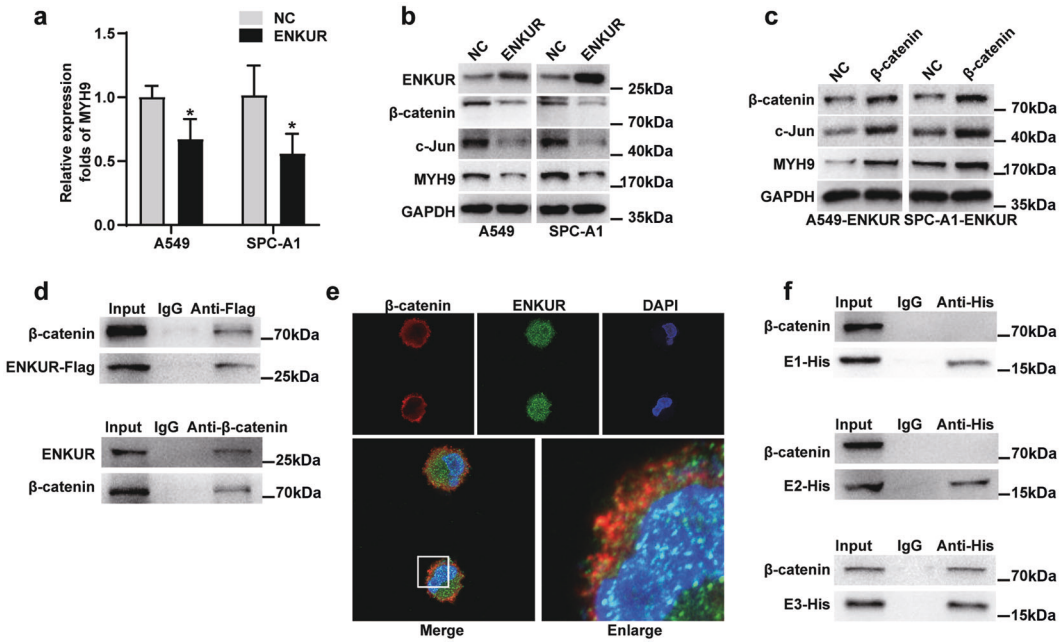

Fig. 4 ENKUR binds to β-catenin to decrease MYH9 expression. a qPCR analysis of MYH9 expression in ENKUR-overexpressing LUAD cells and control cells. **b** The expression levels of β-catenin, c-Jun and MYH9 in ENKUR-overexpressing LUAD cells and control cells. **c** Western blot analysis was used to determine the effects of β-catenin overexpression on the expression of β-catenin, c-Jun and MYH9 in ENKUR-overexpressing LUAD cells. Co-IP (**d**) and immunofluorescence assay (**e**) were used to detect the interaction between ENKUR and β-catenin in ENKUR-overexpressing A549 cells. **f** Co-IP in A549 cells transfected with plasmids containing different domains of ENKUR was utilised to determine the domain that binds to β-catenin.

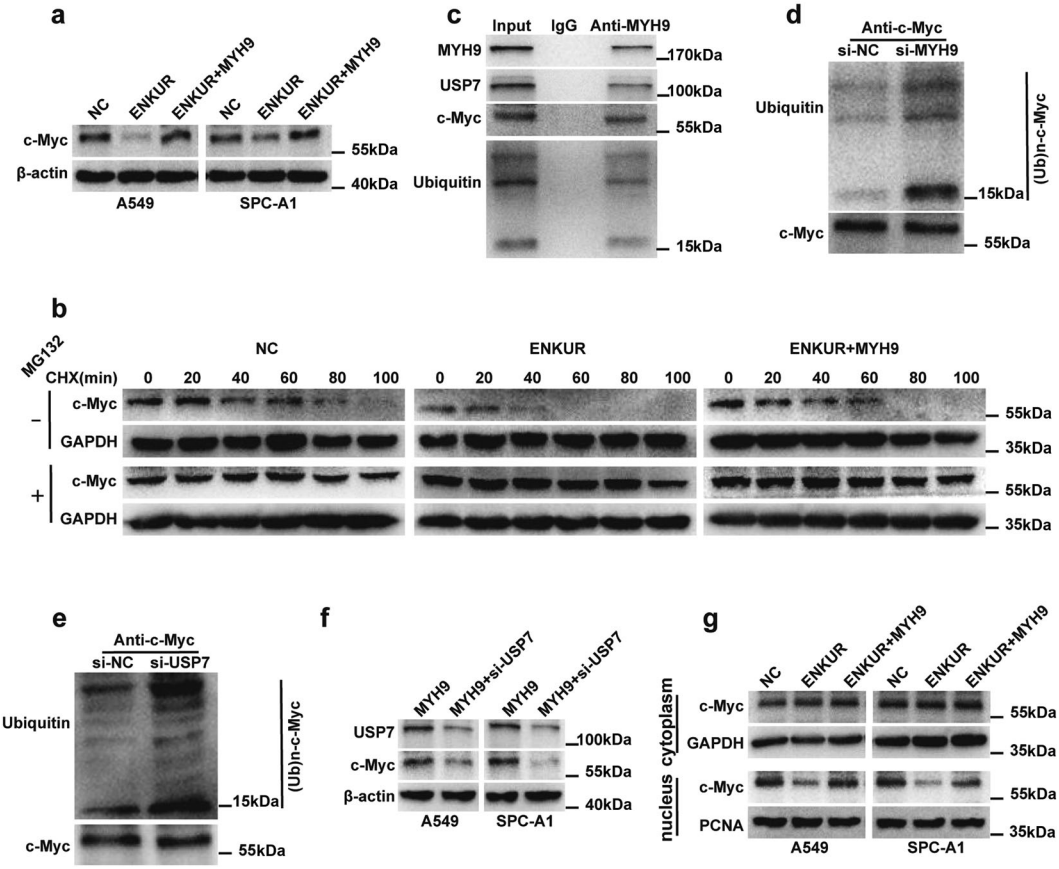

Fig. 5 ENKUR attenuated MYH9/USP7-mediated c-Myc deubiquitination. a Western blot analysis was used to detect the effects of ENKUR and MYH9 on c-Myc protein expression. **b** The effects of ENKUR and MYH9 on the stability of c-Myc are shown in A549 cells incubated with cycloheximide at different time points with or without MG132 treatment. **c** Co-IP assay of the interactions between MYH9, USP7, c-Myc and ubiquitin in A549 cells. **d** and **e** A Co-IP assay was used to detect ubiquitinated c-Myc in MYH9-silenced A549 cells, USP7-silenced A549 cells and the corresponding control cells after treatment with MG132 for 6 h. **f** Western blot analysis was conducted to assess the effect of USP7 depletion on c-Myc expression in LUAD cells transfected with the MYH9 plasmid. **g** The expression of c-Myc in the cytoplasm and nucleus of LUAD cells transfected with the ENKUR or ENKUR + MYH9 plasmid.

epithelial-mesenchymal transition (EMT) signalling in LUAD cells (Supplementary Fig. S4b–e).

ENKUR decreases c-Myc protein expression by suppressing MYH9/USP7-mediated c-Myc deubiquitination

Previous studies have proven that c-Myc activates EMT to promote drug resistance [20]; thus, we hypothesised that c-Myc is the downstream factor of ENKUR that modulates EMT signalling. Decreased c-Myc expression was observed in ENKUR-overexpressing A549 and SPC-A1 cells, while these changes in c-Myc expression were reversed after transfection of the MYH9 plasmid into these cells (Fig. 5a). To determine whether c-Myc is modulated by ENKUR and MYH9 via ubiquitination-mediated degradation, we added CHX to A549 cells transfected with the ENKUR or ENKUR + MYH9 plasmids. The Western blot results showed that ENKUR destabilised the c-Myc protein and that MYH9 restored the stability of c-Myc in ENKUR-overexpressing A549 cells (Fig. 5b). Subsequently, we found that MYH9 interacted with USP7, c-Myc and ubiquitin (Fig. 5c). Knocking down MYH9 and USP7 caused an increase in the level of ubiquitinated c-Myc (Fig. 5d, e). Silencing USP7 decreased the c-Myc protein level in MYH9-overexpressing A549 and SPC-A1 cells (Fig. 5f). The results of nuclear and cytoplasmic fractionation showed that ENKUR decreased c-Myc protein expression in the nucleus and that MYH9 increased c-Myc expression in the nucleus in ENKUR-overexpressing cells (Fig. 5g). Our results indicated that ENKUR increased c-Myc ubiquitination and degradation and inhibited c-Myc nuclear translocation to reduce resistance to DDP.

PI3K/AKT/c-Jun signalling mediates the regulation of ENKUR by CB

C-Jun was predicted to be the transcription factor of ENKUR, with two binding sites, using the JASPAR (http://jaspar.genereg.net) databases (Fig. 6a). The results of qPCR and Western blot analyses showed that the mRNA and protein expression of ENKUR was decreased in c-Jun-transfected A549 and SPC-A1 cells (Fig. 6b, c). Binding of c-Jun to the ENKUR promoter region in A549 and SPC-A1 cells was confirmed by ChIP and gel electrophoresis (Fig. 6d, e). Furthermore, incubation with CB reduced the levels of p-PI3K, p-AKT, and c-Jun and elevated the level of ENKUR in LUAD cells (Fig. 6f). Our data demonstrated that CB induced ENKUR by inhibiting PI3K/AKT/c-Jun signalling-mediated transcription.

CB induces ENKUR expression to overcome DDP resistance

To confirm that upregulated ENKUR mediates the effects of CB to reduce resistance to DDP in LUAD cells, siRNA was used to silence ENKUR expression in CB-treated LUAD cells (Fig. 7a). The data showed that the reduction in DDP resistance and suppression of cell migration and invasion were reversed (Fig. 7b–d). Inhibition of ENKUR upregulated β-catenin, c-Jun, MYH9, c-Myc, and N-cadherin expression and downregulated E-cadherin expression in CB-treated LUAD cells (Fig. 7e). Our results indicated that ENKUR is essential for CB to overcome resistance to DDP in LUAD.

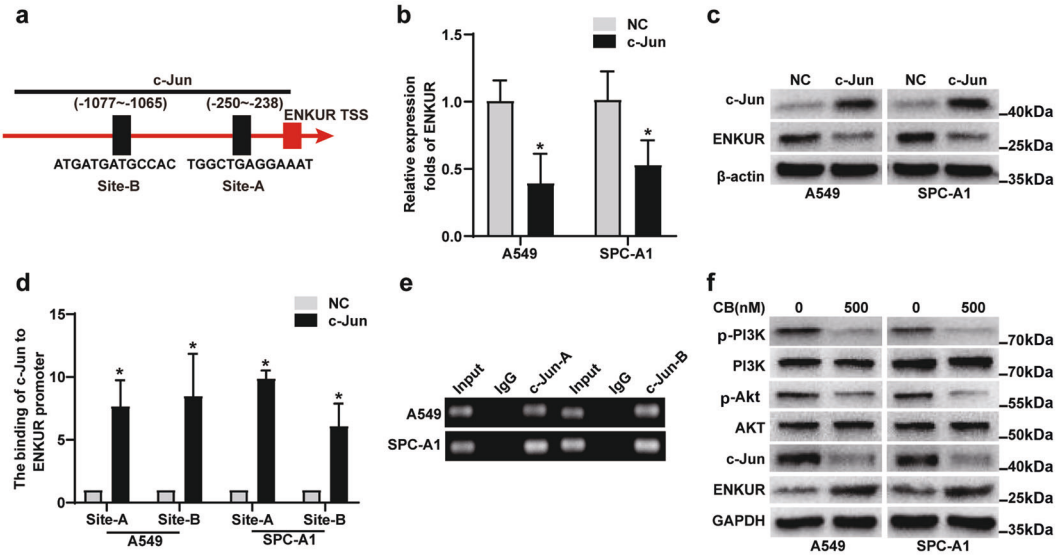

Fig. 6 CB modulates ENKUR via PI3K/AKT/c-Jun signalling. a The binding sites of c-Jun in the ENKUR promoter were predicted by JASPAR. The mRNA (**b**) and protein (**c**) levels of ENKUR were determined in c-Jun-overexpressing LUAD cells and control cells. qPCR assays (**d**) and gel electrophoresis (**e**) after ChIP were used to detect the binding of c-Jun to the ENKUR promoter in A549 and SPC-A1 cells. **f** The levels of p-PI3K, PI3K, p-AKT, AKT, c-Jun and ENKUR in LUAD cells treated with CB.

DISCUSSION

Drug resistance is a great clinical challenge in LUAD treatment and usually leads to a poor prognosis [21, 22]. Once drug resistance occurs, there are fewer chemotherapeutic options for patients with LUAD. Accumulating evidence has shown that EMT is related to chemoresistance and that drug-resistant cells are characterised by enhanced migration and invasion capabilities [23–25]. Our previous studies in NPC demonstrated that CB has potent antitumour activity to decrease resistance to DDP [14, 15]. In the present study, we found that CB reduced the DDP resistance and the migration and invasion abilities of LUAD cells. DDP is the first-line drug for LUAD treatment [26], and treatment experiments in a survival model established by intraperitoneal injection of LUAD cells showed that compared with DDP alone, the combination of CB and DDP contributed to a better prognosis. EMT has been shown to be associated with chemoresistance, migration, and invasion of cancer cells [27, 28]. Subsequently, we proved that suppression of EMT is the mechanism by which CB increases DDP sensitivity and decreases the migration and invasion of LUAD cells. These results indicate that CB is a drug that significantly improves sensitivity to DDP, and its simultaneous use with DDP may be an alternative option for patients with DDP resistance.

ENKUR acts as an adaptor to localise the signal transduction machinery to calcium channels and has been reported to be a tumour suppressor factor in colon cancer and lung cancer [18, 29, 30]. Marinobufagenin was found to increase ENKUR mRNA expression in brain endothelial cells [31]. Since both marinobufagenin and CB are bufagenins and have a similar chemical structure [32], we hypothesised that CB can induce ENKUR expression, thus increasing sensitivity to DDP and reducing the migration and invasion of LUAD cells. Subsequently, we found that the mRNA and protein levels of ENKUR were increased in CB-treated LUAD cells. Overexpression of ENKUR decreased resistance to DDP and inhibited the migration and invasion of LUAD cells. Moreover, in vivo studies showed that the survival time was longest for nude mice treated with ENKUR + DDP, followed by mice in the NC + DDP, ENKUR + NS, and NC + NS groups. To elucidate the mechanism by which ENKUR suppresses LUAD progression, we overexpressed ENKUR in LUAD cells and found decreased β-catenin and N-cadherin expression and increased E-cadherin expression. These results indicated that ENKUR participates in the promotion of DDP sensitivity and inhibition of migration and invasion in LUAD cells by inactivating β-catenin-mediated EMT signalling.

MYH9 has been characterised as a tumour promoter that stimulates EMT in some cancers [33–35]. In this study, we identified MYH9 as an interacting protein of ENKUR and a downstream regulator of ENKUR. Domains are units of proteins and have different functions [36]. The Enkurin domain is essential for interaction with the transient receptor potential-canonical channel [18], and the Myosin_tail domain assembles into a coiled-coil to provide the structural backbone of the thick filament, which is an indispensable component for muscle contraction [37, 38]. Interestingly, we determined that the Enkurin domain of ENKUR binds to MYH9 and the Myosin_tail of MYH9 binds to ENKUR. In addition, MYH9 overexpression restored the suppressive effects of ENKUR on DDP resistance, migration and invasion in LUAD cells. Consistent with previous findings [19], β-catenin/c-Jun signalling-mediated transcriptional regulation was involved in the suppression of MYH9 expression by ENKUR. The deubiquitinase USP7 has been shown to deubiquitinate and thereby stabilise c-Myc to maintain neural stem cell fate [39]. We demonstrated that MYH9 recruits USP7 to deubiquitinate c-Myc, thereby inhibiting the ubiquitination and degradation of c-Myc and promoting its nuclear translocation, leading to increased DDP resistance, migration and invasion in LUAD cells. Our data demonstrated that CB induces ENKUR expression to decrease c-Myc expression by attenuating MYH9/USP7-mediated deubiquitination of c-Myc, identifying a new mechanism by which CB reduces DDP resistance, migration and invasion in LUAD. However, it is not clear how CB stimulates ENKUR expression.

Previous studies have suggested that c-Jun is a transcription factor that regulates the expression of oncogenes and tumour suppressor genes [40–42]. Interestingly, c-Jun was predicted to be a transcription factor of ENKUR. Furthermore, we found that c-Jun binds to the promoter of ENKUR and negatively modulates its expression in LUAD. Emerging evidence has shown that the PI3K/AKT signalling pathway is upstream of c-Jun and participates in tumour progression [43–45]. Subsequently, we proved that PI3K/AKT/c-Jun signalling is involved in the stimulation of ENKUR expression by CB in LUAD. Furthermore, knocking down ENKUR reversed the protein expression pattern and restored the DDP resistance and the migration and invasion abilities of CB-treated cells. These data indicated that CB inhibits the PI3K/AKT/c-Jun/

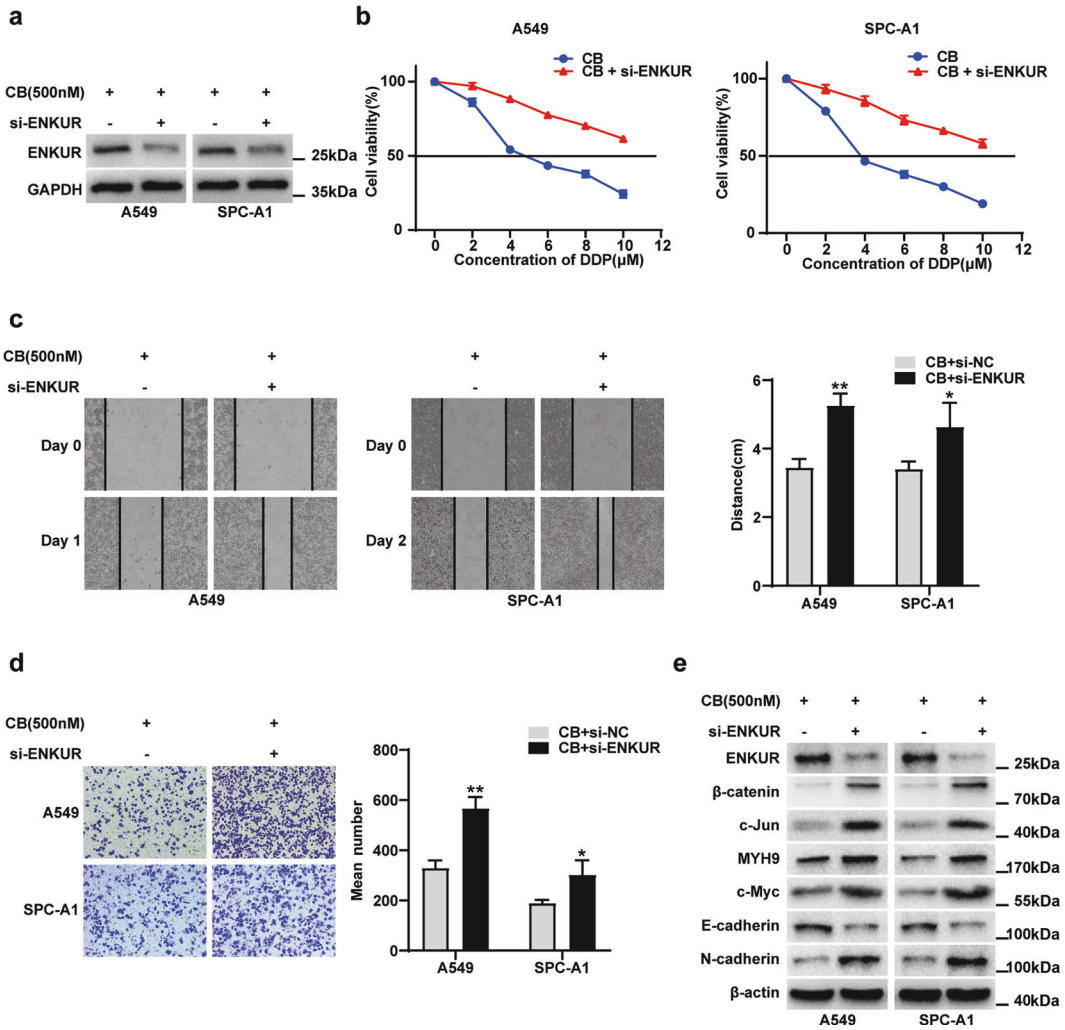

Fig. 7 Knocking down ENKUR reverses the sensitivity of CB-treated cells to DDP. Western blot analysis (**a**), dose–response curves to DDP (**b**), wound healing assays (**c**) and Boyden chamber assays (**d**) were performed in CB-treated LUAD cells transfected with si-ENKUR and the corresponding control cells. **e** The expression levels of ENKUR, β-catenin, c-Jun, MYH9, c-Myc, E-cadherin, and N-cadherin in CB-treated A549 and SPC-A1 cells with or without si-ENKUR transfection are shown.

ENKUR/MYH9 pathway to suppress EMT signalling and thus inhibits DDP resistance in LUAD.

In summary, our data demonstrated the important role of CB in decreasing DDP resistance and the migration and invasion abilities. Furthermore, we clarified the mechanism by which CB inactivates PI3K/AKT/c-Jun signalling to induce ENKUR expression. The upregulated ENKUR not only interacts with MYH9 but also recruits β-catenin to decrease c-Jun-induced transcription of MYH9. MYH9 downregulation reduced the recruitment of USP7 and contributed to the ubiquitination-mediated degradation of c-Myc and suppression of EMT signalling. This work revealed the role of CB in decreasing chemoresistance and its potential application as a chemotherapeutic drug for LUAD patients, especially those with resistance to DDP.

DATA AVAILABILITY

All data are available in this manuscript and supplementary files.

ACKNOWLEDGEMENTS

This study was supported by the National Natural Science Foundation of China (No. 81974460; No. 81572649), Science and Technology Program of Guangzhou (No. 201803010023), Basic Research Project of Guangzhou Municipal Health Committee (No. 2060206), and Natural Science Foundation of Jiangxi Province (No. 20202BAB206077).

AUTHOR CONTRIBUTIONS

WYF, ZL and YBW designed the research. JHL, HLY, STD, WFC, ZH, WWY, RTH, YHL, RTX, YYX, YS, LYW, PX, ZBZ, XL and YLD carried out the experiments and performed the data analysis. JHL wrote the manuscript. WYF revised the manuscript. All of the authors have read and approved the final manuscript.

ADDITIONAL INFORMATION

Supplementary information The online version contains supplementary material available at https://doi.org/10.1038/s41401-022-00890-x.

Competing interests: The authors declare no competing interests.

REFERENCES

1. Sung H, Ferlay J, Siegel RL, Laversanne M, Soerjomataram I, Jemal A, et al. Global Cancer Statistics 2020: GLOBOCAN estimates of incidence and mortality worldwide for 36 cancers in 185 countries. CA Cancer J Clin. 2021;71:209–49.
2. Deng QD, Lei XP, Zhong YH, Chen MS, Ke YY, Li Z, et al. Triptolide suppresses the growth and metastasis of non-small cell lung cancer by inhibiting β-catenin-mediated epithelial-mesenchymal transition. Acta Pharmacol Sin. 2021;42:1486–97.

3. Jordan EJ, Kim HR, Arcila ME, Barron D, Chakravarty D, Gao J, et al. Prospective comprehensive molecular characterization of lung adenocarcinomas for efficient patient matching to approved and emerging therapies. Cancer Discov. 2017;7:596–609.
4. Zhang C, Zhang Z, Zhang G, Zhang Z, Luo Y, Wang F, et al. Clinical significance and inflammatory landscapes of a novel recurrence-associated immune signature in early-stage lung adenocarcinoma. Cancer Lett. 2020;479:31–41.
5. Hirsch FR, Scagliotti GV, Mulshine JL, Kwon R, Curran WJ Jr, Wu YL, et al. Lung cancer: current therapies and new targeted treatments. Lancet. 2017;389:299–311.
6. Thai AA, Solomon BJ, Sequist LV, Gainor JF, Heist RS. Lung cancer. Lancet. 2021;398:535–54.
7. Huang S, He T, Yang S, Sheng H, Tang X, Bao F, et al. Metformin reverses chemoresistance in non-small cell lung cancer via accelerating ubiquitination-mediated degradation of Nrf2. Transl Lung Cancer Res. 2020;9:2337–55.
8. Chen Y, Tang WY, Tong X, Ji H. Pathological transition as the arising mechanism for drug resistance in lung cancer. Cancer Commun. 2019;39:53.
9. Taylor S, Spugnini EP, Assaraf YG, Azzarito T, Rauch C, Fais S. Microenvironment acidity as a major determinant of tumor chemoresistance: proton pump inhibitors (PPIs) as a novel therapeutic approach. Drug Resist Update. 2015;23:69–78.
10. Zhang X, Liu T, Zhang Y, Liu F, Li H, Fang D, et al. Elucidation of the differences in cinobufotalin's pharmacokinetics between normal and diethylnitrosamine-injured rats: the role of P-glycoprotein. Front Pharmacol. 2019;10:521.
11. Sun H, Wang W, Bai M, Liu D. Cinobufotalin as an effective adjuvant therapy for advanced gastric cancer: a meta-analysis of randomized controlled trials. Onco Targets Ther. 2019;12:3139–60.
12. Guo N, Miao Y, Sun M. Transcatheter hepatic arterial chemoembolization plus cinobufotalin injection adjuvant therapy for advanced hepatocellular carcinoma: a meta-analysis of 27 trials involving 2079 patients. Onco Targets Ther. 2018;11:8835–53.
13. Zhang F, Yin Y, Xu T. Cinobufotalin injection combined with chemotherapy for the treatment of advanced NSCLC in China: A PRISMA-compliant meta-analysis of 29 randomized controlled trials. Medicines. 2019;98:e16969.
14. Li Y, Liu X, Lin X, Zhao M, Xiao Y, Liu C, et al. Chemical compound cinobufotalin potently induces FOXO1-stimulated cisplatin sensitivity by antagonizing its binding partner MYH9. Signal Transduct Target Ther. 2019;4:48.
15. Liu Y, Jiang Q, Liu X, Lin X, Tang Z, Liu C, et al. Cinobufotalin powerfully reversed EBV-miR-BART22-induced cisplatin resistance via stimulating MAP2K4 to antagonize non-muscle myosin heavy chain IIA/glycogen synthase 3β/β-catenin signaling pathway. EBio Med. 2019;48:386–404.
16. Zhang J, Luo A, Huang F, Gong T, Liu Z. SERPINE2 promotes esophageal squamous cell carcinoma metastasis by activating BMP4. Cancer Lett. 2020;469:390–8.
17. Liang L, Fu J, Wang S, Cen H, Zhang L, Mandukhail SR, et al. MiR-142-3p enhances chemosensitivity of breast cancer cells and inhibits autophagy by targeting HMGB1. Acta Pharm Sin B. 2020;10:1036–46.
18. Sutton KA, Jungnickel MK, Wang Y, Cullen K, Lambert S, Florman HM. Enkurin is a novel calmodulin and TRPC channel binding protein in sperm. Dev Biol. 2004;274:426–35.
19. Lin X, Li AM, Li YH, Luo RC, Zou YJ, Liu YY, et al. Silencing MYH9 blocks HBx-induced GSK3β ubiquitination and degradation to inhibit tumor stemness in hepatocellular carcinoma. Signal Transduct Target Ther. 2020;5:13.
20. Tao L, Shu-Ling W, Jing-Bo H, Ying Z, Rong H, Xiang-Qun L, et al. MiR-451a attenuates doxorubicin resistance in lung cancer via suppressing epithelialmesenchymal transition (EMT) through targeting c-Myc. Biomed Pharmacother. 2020;125:109962.
21. Yousafzai NA, Zhou Q, Xu W, Shi Q, Xu J, Feng L, et al. SIRT1 deacetylated and stabilized XRCC1 to promote chemoresistance in lung cancer. Cell Death Dis. 2019;10:363.
22. Tang H, Chen J, Han X, Feng Y, Wang F. Upregulation of SPP1 is a marker for poor lung cancer prognosis and contributes to cancer progression and cisplatin resistance. Front Cell Dev Biol. 2021;9:646390.
23. Shen M, Xu Z, Xu W, Jiang K, Zhang F, Ding Q, et al. Inhibition of ATM reverses EMT and decreases metastatic potential of cisplatin-resistant lung cancer cells through JAK/STAT3/PD-L1 pathway. J Exp Clin Cancer Res. 2019;38:149.
24. Lu HY, Zu YX, Jiang XW, Sun XT, Liu TY, Li RL, et al. Novel ADAM-17 inhibitor ZLDI-8 inhibits the proliferation and metastasis of chemo-resistant non-small-cell lung cancer by reversing Notch and epithelial mesenchymal transition in vitro and in vivo. Pharmacol Res. 2019;148:104406.
25. Han Q, Cheng P, Yang H, Liang H, Lin F. miR-146b Reverses epithelial-mesenchymal transition via targeting PTP1B in cisplatin-resistance human lung adenocarcinoma cells. J Cell Biochem. 2019;121:3901-12.
26. Ma YP, Yang Y, Zhang S, Chen X, Zhang N, Wang W, et al. Efficient inhibition of lung cancer in murine model by plasmid-encoding VEGF short hairpin RNA in combination with low-dose DDP. J Exp Clin Cancer Res. 2010;29:56.
27. van Staalduinen J, Baker D, Ten Dijke P, van Dam H. Epithelial-mesenchymal-transition-inducing transcription factors: new targets for tackling chemoresistance in cancer? Oncogene. 2018;37:6195–211.
28. Pastushenko I, Brisebarre A, Sifrim A, Fioramonti M, Revenco T, Boumahdi S, et al. Identification of the tumour transition states occurring during EMT. Nature. 2018;556:463–8.
29. Ma Q, Lu Y, Gu Y. ENKUR is involved in the regulation of cellular biology in colorectal cancer cells via PI3K/Akt signaling pathway. Technol Cancer Res Treat. 2019;18:1533033819841433.
30. Ma Q, Lu Y, Lin J, Gu Y. ENKUR acts as a tumor suppressor in lung adenocarcinoma cells through PI3K/Akt and MAPK/ERK signaling pathways. J Cancer. 2019;10:3975–84.
31. Ing NH, Berghman L, Abi-Ghanem D, Abbas K, Kaushik A, Riggs PK, et al. Marinobufagenin regulates permeability and gene expression of brain endothelial cells. Am J Physiol Regul Integr Comp Physiol. 2014;306:R918–24.
32. Sinhorin AP, Kerkhoff J, Dall'Oglio EL, de Jesus Rodrigues D, de Vasconcelos LG, Sinhorin VDG. Chemical profile of the parotoid gland secretion of the Amazonian toad (Rhinella margaritifera). Toxicon. 2020;182:30–3.
33. Liu L, Ning Y, Yi J, Yuan J, Fang W, Lin Z, et al. miR-6089/MYH9/β-catenin/c-Jun negative feedback loop inhibits ovarian cancer carcinogenesis and progression. Biomed Pharmacother. 2020;125:109865.
34. Wang B, Qi X, Liu J, Zhou R, Lin C, Shangguan J, et al. MYH9 promotes growth and metastasis via activation of MAPK/AKT signaling in colorectal cancer. J Cancer. 2019;10:874–84.
35. Yang B, Liu H, Bi Y, Cheng C, Li G, Kong P, et al. MYH9 promotes cell metastasis via inducing angiogenesis and epithelial mesenchymal transition in esophageal squamous cell carcinoma. Int J Med Sci. 2020;17:2013–23.
36. Light S, Elofsson A. The impact of splicing on protein domain architecture. Curr Opin Struct Biol. 2013;23:451–8.
37. Strehler EE, Strehler-Page MA, Perriard JC, Periasamy M, Nadal-Ginard B. Complete nucleotide and encoded amino acid sequence of a mammalian myosin heavy chain gene. Evidence against intron-dependent evolution of the rod. J Mol Biol. 1986;190:291–317.
38. Taylor KC, Buvoli M, Korkmaz EN, Buvoli A, Zheng Y, Heinze NT, et al. Skip residues modulate the structural properties of the myosin rod and guide thick filament assembly. Proc Natl Acad Sci USA. 2015;112:E3806–15.
39. Nicklas S, Hillje AL, Okawa S, Rudolph IM, Collmann FM, van Wuellen T, et al. A complex of the ubiquitin ligase TRIM32 and the deubiquitinase USP7 balances the level of c-Myc ubiquitination and thereby determines neural stem cell fate specification. Cell Death Differ. 2019;26:728–40.
40. Zou Y, Lin X, Bu J, Lin Z, Chen Y, Qiu Y, et al. Timeless-stimulated miR-5188-FOXO1/β-Catenin-c-Jun feedback loop promotes stemness via ubiquitination of β-catenin in breast cancer. Mol Ther. 2020;28:313–27.
41. Liu Y, Chen X, Cheng R, Yang F, Yu M, Wang C, et al. The Jun/miR-22/HuR regulatory axis contributes to tumourigenesis in colorectal cancer. Mol Cancer. 2018;17:11.
42. Chen S, Zhang J, Yu WB, Zhuang JC, Xiao W, Wu ZY, et al. Eomesodermin in $CD4^+$ T cells is essential for Ginkgolide K ameliorating disease progression in experimental autoimmune encephalomyelitis. Int J Biol Sci. 2021;17:50–61.
43. Liang Z, Liu Z, Cheng C, Wang H, Deng X, Liu J, et al. VPS33B interacts with NESG1 to modulate EGFR/PI3K/AKT/c-Myc/P53/miR-133a-3p signaling and induce 5-fluorouracil sensitivity in nasopharyngeal carcinoma. Cell Death Dis. 2019;10:305.
44. Wang C, Liu E, Li W, Cui J, Li T. MiR-3188 inhibits non-small cell lung cancer cell proliferation through FOXO1-mediated mTOR-p-PI3K/AKT-c-JUN signaling pathway. Front Pharmacol. 2018;9:1362.
45. Yi R, Yang S, Lin X, Zhong L, Liao Y, Hu Z, et al. miR-5188 augments glioma growth, migration and invasion through an SP1-modulated FOXO1-PI3K/AKT-c-JUN-positive feedback circuit. J Cell Mol Med. 2020;24:11800–13.